RESEARCH ARTICLE

Macromolecular Rapid Communications
www.mrc-journal.de

Engineering Nanotrap Hydrogel for Immune Modulation in Wound Healing

*Xiguang Yang, Dandan Guo, Xiaotian Ji, Changying Shi, and Juntao Luo**

Imbalanced immune regulation leads to the abnormal wound healing process, e.g., chronic unhealing wound or hypertrophic scar formation. Thus, the attenuation of the overflowing inflammatory factors is a viable approach to maintain the homeostatic immune regulation to facilitate normal wound healing. A versatile telodendrimer (TD) nanotrap (NT) platform is developed for efficient biomolecular protein binding. The conjugation of TD NT in size-exclusive biocompatible hydrogel resin allows for topical application for cytokine scavenging. Fine-tuning the TD NT density/valency in hydrogel resin controls resin swelling, optimizes molecular diffusion, and improves cytokine capture for effective immune modulation. The hydrogel with reduced TD NT density allows for higher protein/cytokine adsorption capacity with faster kinetics, due to the reduced barrier of TD NT nano-assembly. The positively charged TD NT hydrogel exhibits superior removal of negatively charged proinflammatory cytokines from the lipopolysaccharide (LPS, a potent endotoxin) primed immune cell culture medium. The negatively charged TD NT hydrogel removes positively charged anti-inflammatory cytokines efficiently from cell culture medium. TD NT hydrogel effectively constrains the local inflammation induced by subcutaneous LPS injection in mice. These results indicate the great potential applications of the engineered TD NT hydrogel as topical immune modulatory treatments to attenuate local inflammation.

1. Introduction

The tissue damages in wound release damage associated molecular patterns (DAMPs), which trigger immune cells to secrete signaling molecules, such as cytokines, to initiate inflammatory phase of wound healing process.[1] Impaired wound healing is often associated with prolonged inflammation in disorders related to immune dysregulation, such as diabetes, obesity, and therapy-induced immune-compromised complications.[2] Chronic wounds, such as chronic venous leg ulcers, are characterized by the excessive and prolonged presence of proinflammatory cells and molecules, including proinflammatory cytokines, damage/pathogen associated molecular patterns (DAMPs/PAMPs) at the local environment,[3–5] which lead to persistent inflammation and halt the healing process. The dysregulated inflammatory monocytes/macrophages and neutrophils unrestrainedly produce cytokines and chemokines to recruit more immune cells into the local wound tissue and secrete more tissue-lytic enzymes, e.g., matrix metalloproteinases (MMP), which prevent the healing process.[6,7] On the other hand, patients with severe burn injury usually suffer from persistent systemic inflammation and can develop hypertrophic scar formation, resulting from the high level of transforming growth factor β (TGF-β).[8–10] TGF-β stimulates fibroblasts and myofibroblasts to produce high amounts of collagen and other extracellular matrix (ECM) components, forming fibrotic tissue in pathological scars.[11,12] Thus, attenuation of TGF-β is considered a valid approach to prevent pathological scars.[13,14]

Numerous therapeutic approaches have been established to alleviate local inflammation, including the employment of anti-inflammatory agents like corticosteroids,[15] and monoclonal antibodies that target inflammatory cytokines.[16] Another strategy involves functional materials developed for scavenging key immune-stimulating molecules, such as monocyte chemoattractant protein-1 (MCP-1), tumor necrosis factor-alpha (TNF-α), and interleukin-8 (IL-8),[6,17] or reactive oxygen species (ROS) from the chronic wound environment.[18–20] However, these therapies have limitations in terms of efficacy due to their adverse effects, drug resistance, and high costs. To resume the healing process, novel biocompatible functional materials with immune modulation capabilities that balance local hemostasis are required.

X. Yang, D. Guo, X. Ji, C. Shi, J. Luo
Department of Pharmacology
State University of New York Upstate Medical University
Syracuse, NY 13210, USA
E-mail: luoj@upstate.edu

J. Luo
Department of Surgery
State University of New York Upstate Medical University
Syracuse, NY 13210, USA

J. Luo
Department of Immunology and Microbiology
State University of New York Upstate Medical University
Syracuse, NY 13210, USA

J. Luo
Upstate Cancer Center
State University of New York Upstate Medical University
Syracuse, NY 13210, USA

J. Luo
Upstate Sepsis Interdisciplinary Research Center
State University of New York Upstate Medical University
Syracuse, NY 13210, USA

The ORCID identification number(s) for the author(s) of this article can be found under https://doi.org/10.1002/marc.202300322

DOI: 10.1002/marc.202300322

We have developed a well-defined telodendrimer (TD) nanotrap (NT) platform, which can be customized for both drug and protein encapsulation.[21–23] The synergistic combination of multiple adjacent charges and hydrophobic moieties in dendritic TD enables effective surface coating on biomolecules independent of molecular conformations. The conjugation of TD NT in size-exclusive polyethylene glycol acrylamide (PEGA) based co-polymer hydrogel resin has resulted in a versatile PEGA-NT platform for adsorption of a broad range of pathogenic septic molecules and proinflammatory cytokines in sepsis treatment.[24] Our objective in this study is to extend the application of the TD NT platform for topical immune modulation therapy, i.e., chronic wound treatment. Wound dressing containing TD NT resins can serve as an efficient local scavenger, sequestering high amounts of inflammatory mediators from the unhealing wounds to resolve the inflammatory process. Although we have previously demonstrated the efficacy of PEGA-NT resins for immune modulation therapy,[24,25] the density and valency of TD NT in hydrogel resin have not been studied systematically, which directly impact the binding affinity, as well as the binding kinetics, due to the alteration of hydrophilicity and swelling properties, thus influencing molecular diffusion, especially for biomacromolecules. Here, we systematically synthesized PEGA-NT resins with different TD NT densities and valencies, incorporating both positively and negatively charged moieties to optimize the scavenging of different cytokines in vitro and in vivo. The scavenging efficiency of the materials was compared in capture assay using model protein, conditioned medium containing a mix of immune cell-derived inflammatory cytokines. A mouse model with lipopolysaccharide (LPS) induced inflammation was applied to evaluate the overall local immune-regulation with PEGA-NT hydrogel for potential wound treatment.

2. Results and Discussion

2.1. PEGA-NT Resin Engineering and Characterization

Telodendrimer (TD) nanotrap (NT) conjugated in the commercial polyethylene glycol acrylamide (PEGA) resin has proved effective in scavenging septic molecules, such as endotoxin, DAMPs/PAMPs, and inflammatory cytokines in sepsis treatment.[24] In this study, we aim to further optimize TD NT in PEGA resin and evaluate the application into topical usage for effective immune modulation. The molecular diffusion into a hydrogel depends on the size of the analytes and the pore size of hydrogel network, which is determined by the crosslinking and swelling properties. The commercial PEGA resins have size exclusive effect against protein molecules with molecular weight >40–50 kDa,[26] thus allowing for effective scavenging of most signaling molecules, which generally have small–medium sizes (10–30 kDa). However, the introduction of TD NT impacts the swelling of PEGA resin due to the reduced hydrophilicity, as well as the self-assembly of TD NT into nano-domains as additional physical cross-linking. As conceptualized in **Figure 1**A, the density and the valency of TD NT in PEGA resin need to be fine-tuned to control the hydrogel swelling for effective molecular diffusion and optimal molecular binding.

As observed in our previous study, the commercial hydrogel PEGA resin shrinks after conjugation of TD at full functional capacity. Thus, we decided to downscale the density of functional amine groups in PEGA resin before TD synthesis by quantitative partial amine-blocking as shown in Scheme S1 (Supporting Information). Briefly, amino-PEGA resins were coupled with a mixture of orthogonally protected glycine, i.e., Fmoc-glycine and Boc-glycine, at a predetermined ratio. Following the standard peptide chemistry, Fmoc protection group on PEGA resin can be selectively deprotected with base and qualified via UV–vis absorbance at 301 nm (Figure 1B). Then, the free amine groups were permanently blocked by acetic anhydride to reduce available functional groups. Then Boc protected glycine on resin will be deprotected by acidic treatment to expose free amine groups for TD synthesis on resin. Accordingly, we have downscaled a series of PEGA resins with the capacity of 1%, 5%, 10%, 25%, 50%, and 100% to the original loading capacity. The UV-vis quantification analysis revealed that the downscaled PEGA resins have amine group density close to the designed values at 2.7%, 8.1%, 13.7%, 27.8%, 58.1%, and 103.9%, respectively, to the original loading capacity (0.33 mmol g^{-1}). The slightly higher measured capacity could be attributed to the systemic error, as well as the fact that Boc-glycine has smaller size for diffusion and higher reactivity for less stereo hindrance compared to the Fmoc-glycine.

In addition to the passive diffusion, the binding affinity of the analytes with the ligand and polymer matrix also impacts the adsorption rate,[27,28] as well as the retention and release of the analytes. The backbone of PEGA resin mainly consists of hydrophilic polyethylene glycol and polar polyacrylamide, which have weak interactions with drugs and biomolecules in the aqueous solution. In contrast, the specifically designed TD NT immobilized in hydrogel provides a strong binding affinity to these molecules through a multivalent and synergistic combination of charge and hydrophobic interactions.[22] The binding site barrier may be also applicable for TD NT PEGA resin, as observed for the high-affinity antibodies with limited tissue and tumor penetration.[29] Thus, we adjusted the valency of TD as well (Figure 1A) to fine-tune the binding affinity to drug or protein molecules in the hydrogel to optimize the protein adsorption kinetics. The combinations of either negative carboxylic acid (COOH) or positive Arginine (Arg) groups with hydrophobic heptadecanoic acid (C17) moieties in TD have demonstrated the synergy for effective protein delivery and bio-scavenging for immune modulation,[21–25] thus were selected as functional moieties to be synthesized on PEGA-NT resins with different valency and density to fine-tune the swelling property. The stepwise conjugation of TD NT on commercial PEGA hydrogel resin has been described in our previous work following the standard solid-phase peptide synthesis via standard Fmoc/Boc chemistry.[24] The detailed synthetic routes of TD NT on PEGA resin are shown in the Scheme S1 (Supporting Information). The completion of each amine coupling during TD synthesis was monitored by the chromogenic Kaiser test for quality control. As shown in Figure 1C, the decreased amine and TD density in resin was reflected by the gradually reduced blue color in Kaiser test. After amide coupling, protecting groups were cleaved to expose the charged groups, e.g., COOH or guanidine. The engineered resins were thoroughly washed with organic solvents to remove unreacted reagents, dried and stored in the refrigerator.

As expected, TD density has a great impact on the swelling of PEGA resins with the decreased swelling volume in water for the

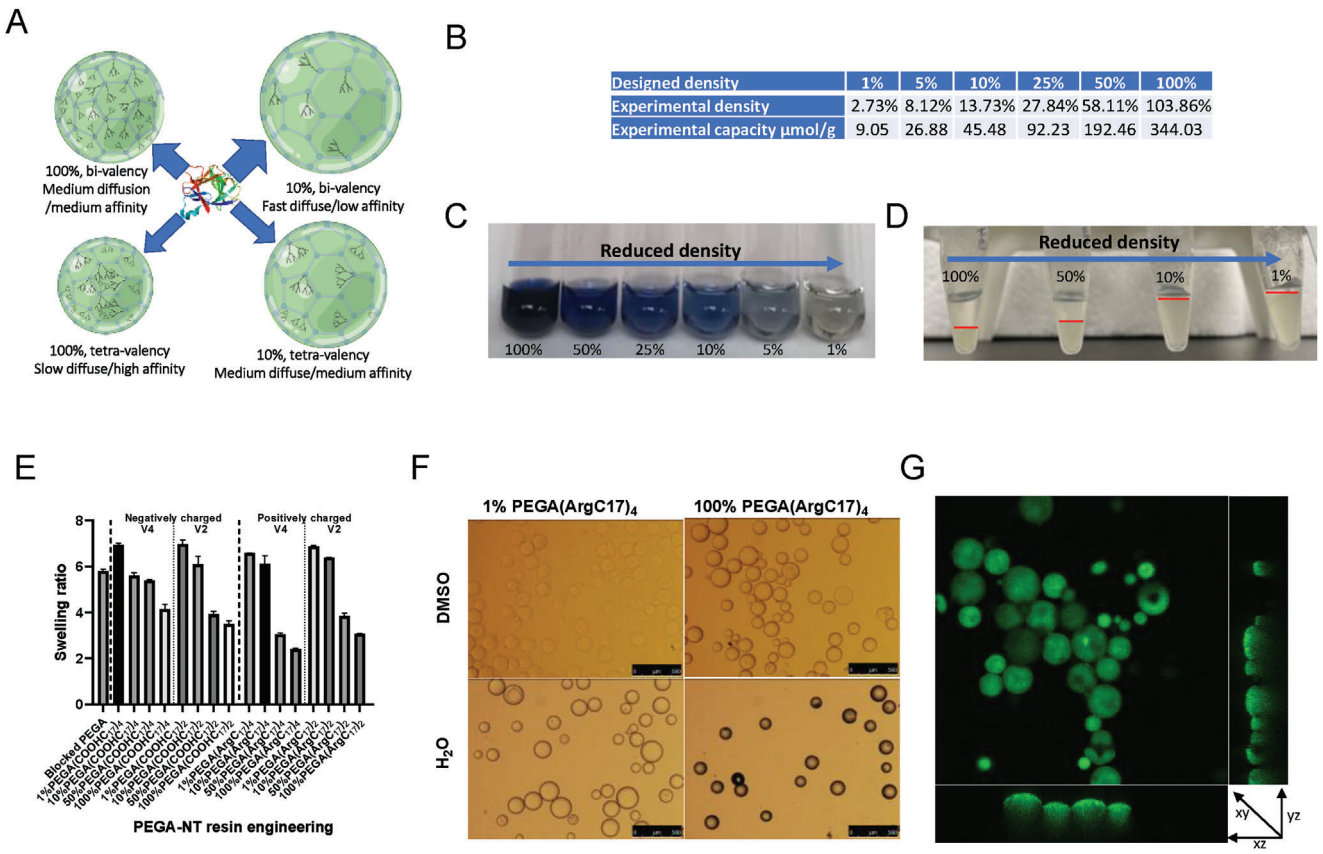

Figure 1. PEGA-NT resin engineering and physical properties characterization. A) Schematic illustration of resin swelling properties related to the different density and valency of TD NT, the branched structure conjugated in the sphere represents TD NT. B) The downscaling of density of amine groups in PEGA resin can be quantified by UV–vis spectroscopy using the characteristic wavelength of the Fmoc group at 301 nm. C) Darkness of the blue color in Kaiser test of amino-PEGA resin indicates the gradually decreasing free amine groups in resins after blocking certain percent of amine groups. D) The swelling properties of PEGA-NT resins increases with the reduced density of the conjugated TD$(ArgC17)_4$. E) The swelling properties (ratio of wet to dry weight) of engineered PEGA resins with different density and valency of TD NT. F) Representative microscopy images showed different swelling behavior of PEGA resin with different density of TD in two solvents, DMSO (dimethyl sulfoxide) and water. Scale bar: 500 μm. G) 3D confocal microscope images of FITC conjugated PEGA resins indicates homogenous functional group distribution after downscaling the loading capacity of original amine groups in PEGA resin.

same weight of resin (Figure 1D). The quantitative swelling ratio of resins are shown in Figure 1E, blank PEGA resin swells significantly in PBS with an increased wet weight about six-fold relative to the dry weight. The PEGA resin with 50%–100% TD density show significantly reduced swelling with 30%–50% reduction in comparison to the blank PEGA. In contrast, PEGA resins with 1%–10% of TD density swell similarly to the blank PEGA even with a slight increase, which is likely due to that low TD density interfere PEG chain interactions via hydrogel bonding, resulting in even slightly increasing PEGA swelling. This data is indicative of the additional physical crosslinking caused by the high-density TDs, facilitating self-assembly due to their proximity. Interestingly, TDs with bi-valency or tetra-valency have similar swelling properties, indicating that density determines the critical distance between TDs in PEGA resin for TD assembly. The positively charged TD$(ArgC17)_4$ exhibits the most reduction in resin swelling compared with negatively charged TD$(COOHC17)_4$ at the high density, likely due to that guanidine group in Arg groups form stronger hydrogel bonding with PEG chain by providing more protons as compared with COOH in negative TD. Further, we validate swelling properties under light microscope after soaking PEGA-NT resins in DMSO and water. As shown in Figure 1F and Figure S1A (Supporting Information), the PEGA-NT resins swell similarly in DMSO solvent regardless of their TD density due to the amphiphilic feature of DMSO; while PEGA-NT resins swell dramatically differently in water: higher density of TD resins swell less, indicating the TD moieties induce resin shrinking in water at higher density with more hydrophobic moieties. In addition, confocal microscopy showed that FITC fluorescent dye is homogeneously conjugated within the PEGA resin via free amines, suggesting homogenous downscaling of functional groups in resin (Figure 1G; Figure S1B, Supporting Information).

2.2. Protein Capturing Property of PEGA-NT Resin

Protein adsorption in PEGA-NT resin depends on the protein sizes, charge density, and hydrophobicity, as well as the TD NT properties in resin, e.g., chemical structure, valency, and density.

We selected two model proteins with similar molecular weights, but distinct charges to mimic cytokines, i.e., α-LA (MW: 14 kDa, PI: 4.2) and lysozyme (MW: 14 kDa, PI: 11.4), to test the capture properties of engineered TD NT resins. Interestingly, the majority of pro-inflammatory cytokines have negative charges, e.g., tumor necrosis factor-α (TNF-α), interleukin-1 beta (IL-1β), interleukin-6 (IL-6); and major anti-inflammatory cytokines, e.g., interleukin-10 (IL-10), interleukin-4 (IL-4), and transforming growth factor beta (TGF-β), are positively charged.[4,30] Thus α-LA and lysozyme can mimic pro- and anti-inflammatory cytokines in this study, respectively. Accordingly, COOH and Arg in PEGA resins were applied to capture these two model proteins. Model proteins were conjugated with fluorescent dye to facilitate the concentration measurement in resin incubated solution by fluorescent spectrometry. As controls, PEGA resins with TD structures possessing only charges (positive or negative), only hydrophobic moieties, and PEGA resin with acetylated amine groups were included for comparison.

As shown in **Figure 2**A, both density and valency of the positively charged TD(ArgC17) in PEGA resins have impact on the kinetics and capturing efficiency of the negatively charged protein Cy3-α-LA. Interestingly, PEGA resins with 10% tetravalent TD$(ArgC17)_4$ and 50% bivalent TD$(ArgC17)_2$ exhibit the optimal Cy3-α-LA capturing properties. While resins with ultra-low 1% TD density fail to capture protein like the blank resin, thus were excluded for further cytokine scavenging evaluation. We quantify protein loading capacity after equilibrium in PEGA resins with different TD moieties (Figure 2B). First, we found PEGA resins with only charge moieties (10% PEGA$(COOH)_2$ and PEGA$(Arg)_2$) have no noticeable protein capture capacity (Figure 2B) as well as the blank PEGA; whereas the resins with the same density of hydrophobic moieties, e.g., 10% PEGA$(C17)_2$, capture significant amount of protein based on hydrophobic interactions. Further, the combination of negative charges with hydrophobic moieties in 10% PEGA$(COOHC17)_4$ cannot further improve the loading capacity of negatively charged α-LA, in comparison to hydrophobic only resin. However, the positively charged 10% PEGA$(ArgC17)_2$ significantly increased α-LA capture capability from 1.6 to 2.8 μg mg^{-1}, indicating the critical charge selectivity and synergistic charge/hydrophobic combination for effective protein capture. Bivalent TD NT PEGA resins with 10%, 50%, or 100% TD densities show similar α-LA loading capacity; whereas the PEGA resin with tetravalent TD reveals a reverse correlation of TD density with the protein loading capacity. Especially, 100% tetravalent TD$(ArgC17)_4$ resin exhibits slower protein adsorption and lowest loading capacity (Figure 2A,B), likely due to the reduced swelling property as shown in Figure 1E. We also applied electrophoresis to evaluate whether the captured protein will reversibly release out from resin. As shown in Figure S2 (Supporting Information), no protein leakage was observed, indicating the strong protein binding affinity for effective immune modulation.

We further evaluate the capturing efficiency of positively charged Cy3-lysozyme in PEGA-NT resins as a surrogate of the majority of anti-inflammatory cytokine. As expected, the lysozyme capture in PEGA-NT resins with 1% density is limited as shown in Figure 2C,D. Interestingly, no significant difference in both kinetics and loading capacity for lysozyme capture in other engineered PEGA(COOHC17) resins, regardless of the density and valency. Similarly, PEGA-NT with only charge moieties cannot capture lysozyme. And hydrophobic PEGA$(C17)_2$ shows significant protein loading capacity, which can only be further improved by the combination of negative charges, indicating charge selectively. As shown in Figure 2E, blank and charge only resin barely absorbs any Cy3-lysozyme molecules (<10%) over time. 10% PEGA$(ArgC17)_4$ adsorb 20% Cy3-lysozyme, the 10%PEGA$(C17)_2$ adsorb 35% Cy3-lysozyme, while the 10% PEGA$(COOHC17)_2$ adsorb >60% Cy3-lysozyme from the solution with fast initial adsorption. Further, we introduce more negative charge species, e.g., squaric acid (SA), phosphate (Phos) to compare with COOH for lysozyme capturing in 10% engineered PEGA-NT resins. 10% PEGA$(ArgC17)_4$ was included as a control resin. As shown in Figure 2F, all engineered resins with negatively charged groups show comparable level of protein capture ranging from 2.2 to 3.2 μg mg^{-1}.

2.3. Proinflammatory Cytokine Removal In Vitro

The attenuation of proinflammatory cytokines is a promising approach to modulate immune status.[24] Here, we apply the engineered PEGA-NT in scavenging pathogenic molecules, such as proinflammatory cytokines, DAMPs, and other small-medium sized inflammatory factors. As illustrated in **Figure 3**A, we used an in vitro inflammation model in RAW 264.7 cell culture with the stimulation with endotoxin lipopolysaccharide LPS (50 ng mL^{-1}) or DAMPs (100 μg mL^{-1}) from Panc-02 cell lysate. After overnight incubation, the proinflammatory cytokines-enriched culture medium was harvested for PEGA-NT resins incubation. Adsorption of representative proinflammatory cytokines, including tumor necrosis factor alpha (TNF-α) and interleukin-6 (IL-6), by various engineered resins was measured by ELISA assay. Consistent with the model protein capture results (Figure 2A), 10% PEGA$(ArgC17)_{2\&4}$ resins have the most efficient cytokine scavenging from LPS stimulated culture medium (LCM), with 75% removal efficiency for TNF-α (Figure 3B) and ≈100% for IL-6 removal (Figure 3C), owing to the superior swelling properties and effective protein binding. In comparison, the removal efficiency was decreased with the TD density of 50% and 100%. Also, the bivalent PEGA$(ArgC17)_2$ performs better than the tetravalent resins for both TNF-α and IL-6 adsorption, due to the different swelling properties. In contrast, blank PEGA resins show almost no effective TNF-α and IL-6 removal (Figure 3B). As shown in Figure 3D, DAMPs induce a low, but significant amount of TNF-α in the DAMP stimulated culture medium (DCM), which mimics the aseptic tissue damage in wound. Consistently, 10% PEGA$(ArgC17)_4$ resins remove TNF-α from DCM more efficiently than other PEGA-NT resins with higher density (Figure 3D). In addition, all 10% PEGA(ArgC17) resins with mono, double valency could remove TNF-α from DCM completely, due to the better resin swelling for TNF-α diffusion. These results suggest that the cytokine scavenging efficiency of PEGA-NT resins can be significantly improved by downscaling the TD density in the PEGA-NT resins.

To further optimize the cytokine scavenging efficiency, conditions, such as temperature, duration, and resin usage were evaluated. It is expected that prolonged incubation and higher temperature allow cytokine molecules to have better chance to

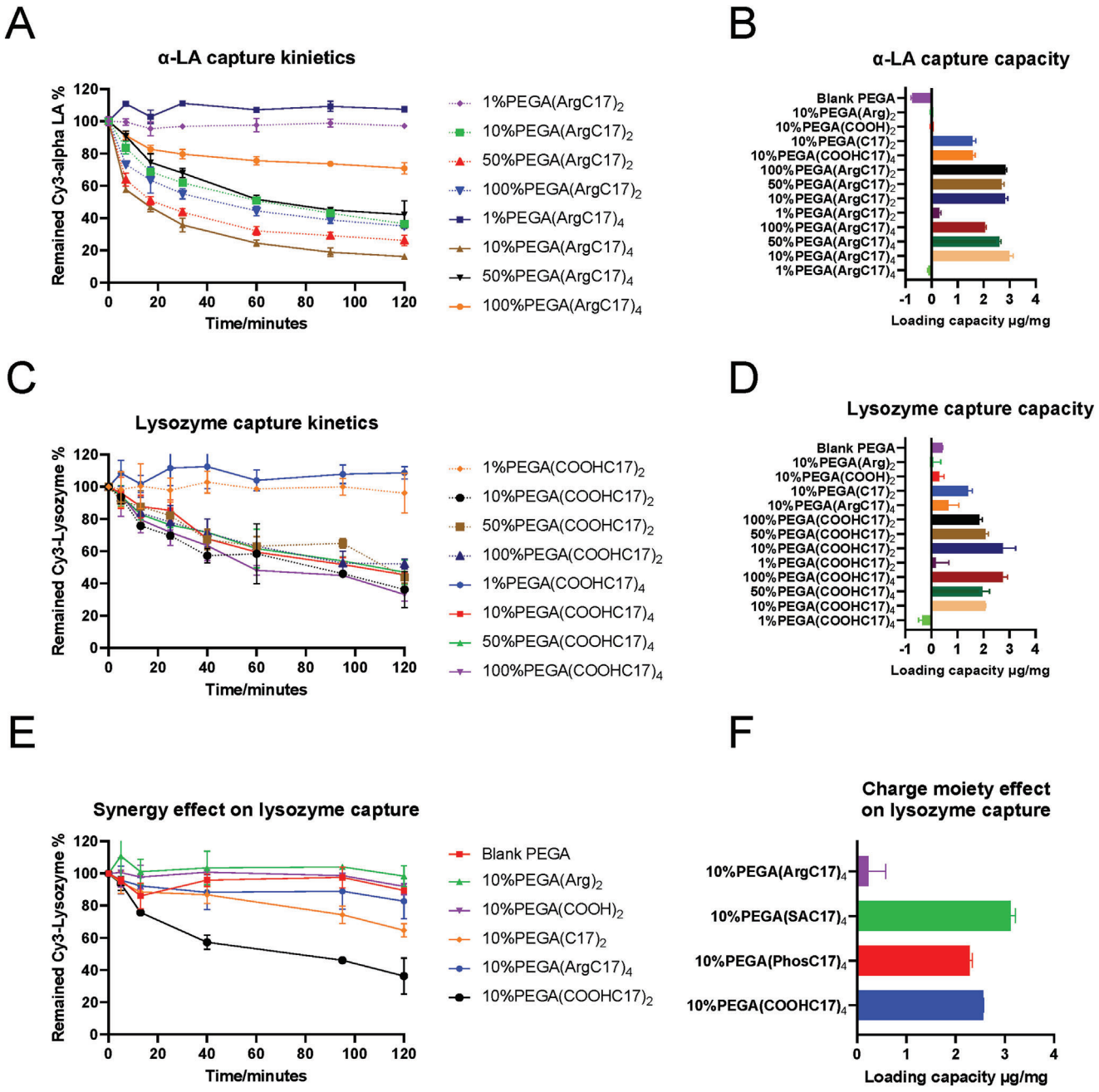

Figure 2. Protein capture kinetics and capacity can be optimized through PEGA-NT engineering. A) Using Cy3 labeled α-lactalbumin, protein capture kinetics was compared between positively charged PEGA-NT resins engineered to different density (1%, 10%, 50%, and 100%). B) Endpoint quantification of α-LA protein capture capacity of engineered PEGA-NT resins. C) Using Cy3 labeled lysozyme, protein capture kinetics was compared between negatively charged PEGA-NT resins engineered to different density (1%, 10%, 50%, and 100%). D) Endpoint quantification of lysozyme capture capacity of engineered PEGA-NT resins. E) Using Cy3 labeled lysozyme, protein capture kinetics was compared between PEGA-NT resins engineered to different moieties (charge only and hydrophobic only). F) Lysozyme capture capacity in PEGA resins with varied negative charge moieties (COOH, SA, and Phosphate) was compared, with PEGA(ArgC17)$_4$ serving as a control group.

interact with TD NT in the resin. As shown in Figure 3E, 10% PEGA(ArgC17)$_4$ outperformed other engineered resins and performed optimally at 20 °C with 16 h incubation with 86% TNF-α removal. In addition, the TNF-α removal is dependent on the resin amount increased from 2 to 10 mg after 2 h incubation (Figure 3F). More intriguingly, usage as little as 2 mg of dry 10% PEGA(ArgC17)$_4$ resins efficiently remove IL-6 with a ≈100% efficiency (Figure 3E), and the dose dependency was also observed in 50% PEGA(ArgC17)$_4$, but not significant in highest density 100% PEGA(ArgC17)$_4$.

In order to analyze protein scavenging capacity of different resins, we characterized LPS-conditioned RAW 264.7 cell

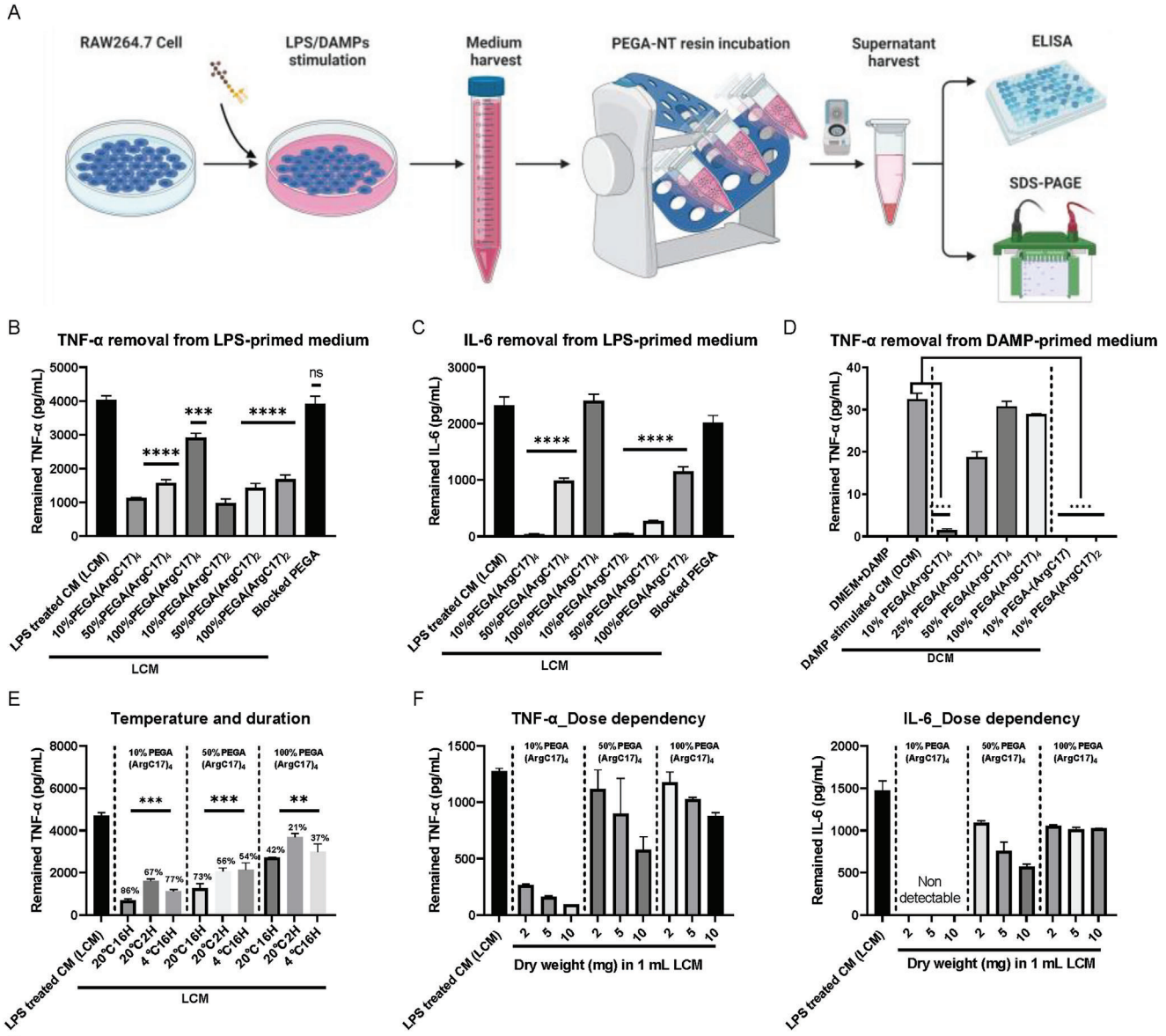

Lane	Samples	L/U	%
1	LPS stimulated Culture Medium	1.74	100.00
2	LCM+100%PEGA(ArgC17)4	1.63	94.01
3	LCM+100%PEGA(ArgC17)2	1.25	72.02
4	LCM+50%PEGA(ArgC17)4	1.69	97.19
5	LCM+50%PEGA(ArgC17)2	**0.74**	**42.84**
6	LCM+10%PEGA(ArgC17)4	1.47	84.64
7	LCM+10%PEGA(ArgC17)2	**1.02**	**58.84**
8	LCM+1%PEGA(ArgC17)4	1.70	98.09
9	LCM+1%PEGA(ArgC17)2	1.72	98.95

Figure 3. Optimization of in vitro pro-inflammatory cytokine scavenging through PEGA-NT engineering. A) Experimental protocol scheme of the cytokine removal assay. RAW 264.7 cells are seeded and challenged by endotoxin LPS (50 ng mL^{-1}) or DAMP (100 μg mL^{-1}) for 24 h. The culture medium is collected as the proinflammatory cytokine enriched culture medium. The medium is aliquoted and incubated with PEGA-NT resins for overnight. The resin-free supernatant is analyzed by ELISA or SDS-PAGE assays. B) Engineered NT resins scavenges proinflammatory cytokines TNF-α or C) IL-6 from LPS treated culture medium and D) DAMP treated culture medium. E) Cytokine removal efficiency optimization by temperature and duration, and F) resin usage. G) Silver stained SDS-PAGE gel indicates superior removal effect of PEGA-NT resins with lower density in adsorbing small to moderate sized proteins from serum free LPS cell culture medium (lane 1).

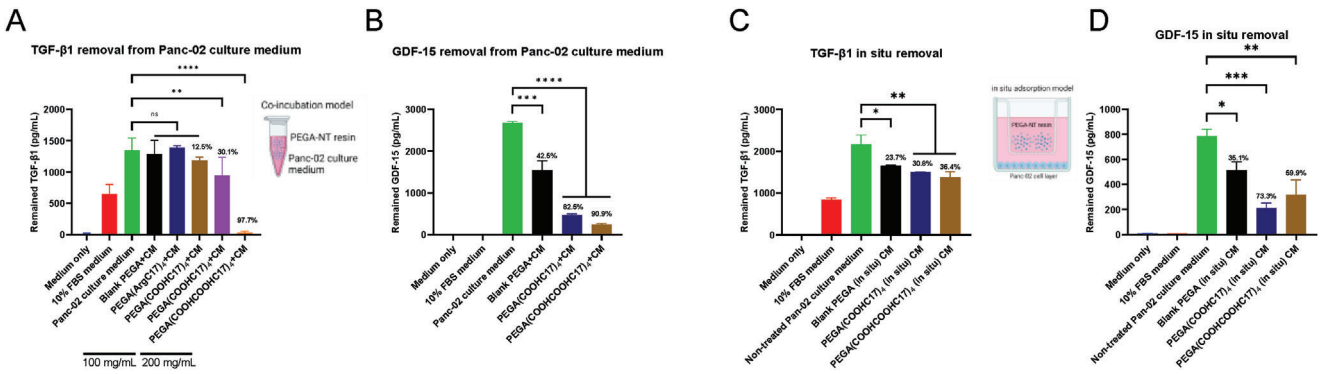

Figure 4. Optimization of in vitro anti-inflammatory cytokine scavenging through PEGA-NT engineering. A) PEGA-NT resins scavenges anti-inflammatory cytokines TGF-β1 and B) GDF-15 from Panc-02 cell culture medium. C) PEGA-NT resins were co-incubated with Panc-02 cell culture using trans-well plate and TGF-β1 and D) GDF-15 levels were measured by ELISA.

medium before and after resin incubation using SDS PAGE with highly sensitive silver staining.[31] To eliminate the background from abundant serum proteins, serum-free culture medium was used during LPS stimulation to harvest inflammatory medium for incubation with PEGA-NT resins. As shown in Figure 3G, it is noticeable that the band intensity of small to moderate sized proteins (10 to 40 kDa) was visually reduced after incubation with the engineered resins for overnight. Especially, the samples treated with 10% PEGA-NT resins show significantly reduced lower band intensity. Large serum proteins have minimum adsorption in PEGA-NT resins due to size-exclusive effects of PEGA resins as demonstrated in our previous study.[24] Therefore, the upper bands (≈75 kDa) were used to normalize the intensity of lower bands (10–37 kDa) as shown in the table of Figure 3G. Untreated LPS stimulated cell culture medium (lane 1) was used for comparison with a L/U ratio of 1.74. The 50% PEGA(ArgC17)$_2$ resins showed the lowest intensity ratio of 0.74 (42.8% to positive control), followed by the 10% PEGA(ArgC17)$_4$ resin of 1.02 (58.8% of positive control). It indicated that 50% PEGA-NT has high capacity in scavenging protein mixtures with small molecular weights, including cytokines, more efficiently from culture medium, while 10% PEGA-NT resin scavenge single cytokine most efficiently. In contrast, 1% PEGA(ArgC17)$_{2\&4}$ resins have limited adsorption in lower molecular weight proteins, as evidenced by the high intensity of the lower bands (1.72 and 1.70). Although, it is not possible to identify individual cytokines, e.g., TNF-α and IL-6, in the silver-stained SDS PAGE gel due to the low abundance, the reduced band intensity for small–medium sized proteins by the engineered TD NT resins provide strong evidence for effective scavenging for potential immune modulation.

2.4. Anti-Inflammatory Cytokine Removal In Vitro

Immunity is known as a double-edged sword regulated at both cellular and molecular levels. In addition, disease progression is usually dynamic with heterogeneous etiology. Phase-dependent customized medicine is a promising approach to immune therapy. To target different phases of wound healing, here we further expand our toolbox by investigating our engineered-NT resins for potential scavenging anti-inflammatory/pro-healing cytokines, which can be pathogenic in hypertrophic scar formation.[11,12] Transforming growth factor beta 1 (TGF-β1) is often chronically over-expressed in disease states, including cancer, fibrosis, and inflammation.[32] Growth/differentiation factor-15 (GDF-15), a TGF-β superfamily protein, was first identified as macrophage inhibitory cytokine-1 (MIC-1) and exerts anti-inflammatory effects.[33] Therefore, we evaluate the scavenging of TGF-β1 (MW: 44.3 kDa, PI: 8.83) and GDF-15 (MW: 34 kDa, PI: 9.79) via the engineered negatively charged PEGA-NT resins. We harvested TGF-β1 and GDF15 enriched culture medium from pancreatic cancer cells Panc-02, which secrete anti-inflammatory (pro-healing) cytokines without exogenous stimulation. As shown in **Figure 4**A, fetal bovine serum (FBS) contains a high level of TGF-β1 (600 pg mL^{-1}) for proliferative effect essential for cell growth. Panc-02 cell culture medium contains elevated levels of TGF-β1 (1600 pg mL^{-1}). Negatively charged PEGA(COOHC17)$_4$ resins remove 12.5% of TGF-β1 from Panc-02 culture medium, and the efficiency increases to 30.1% as the resin usage doubles. Surprisingly, PEGA(COOHCOOHC17)$_4$ with eight charges showed significantly higher efficiency (97.7%) in TGF-β1 scavenging. In contrast, blank PEGA resins and positively charged PEGA(ArgC17)$_4$ resins cannot absorb TGF-β1 as expected. Similarly, in GDF-15 removal as shown in Figure 4B, PEGA(COOHCOOHC17)$_4$ resin showed the highest efficiency of 91%, followed by PEGA(COOHC17)$_4$ with an 83% efficiency, consistent with their superior efficiency in TGF-β1 scavenging. However, it is notable that blank PEGA also removes GDF-15 with 43% efficiency, possibly due to the non-specific adsorption.

In parallel, we conducted an in situ adsorption assay to assess the effectiveness of long-term incubation with engineered PEGA-NT. As shown in Figure 4C,D, treatment with PEGA(COOHCOOHC17)$_4$ removed 36% of TGF-β1 and 60% of GDF-15 from the cell culture, while PEGA(COOHC17)$_4$ exhibited 31% and 73% removal efficiency. The blank PEGA resin showed a removal efficiency of 24% and 35%. The reduced removal efficiency in in situ cell culture assay compared to the culture medium co-incubation model are likely due to the continuous secretion of cytokines, which may saturate the capacity of PEGA-NT. The efficient scavenging of anti-inflammatory cytokines indicates the potential use of PEGA-NT as a tool for therapy of fibrosis, and hypertrophic scar formation.

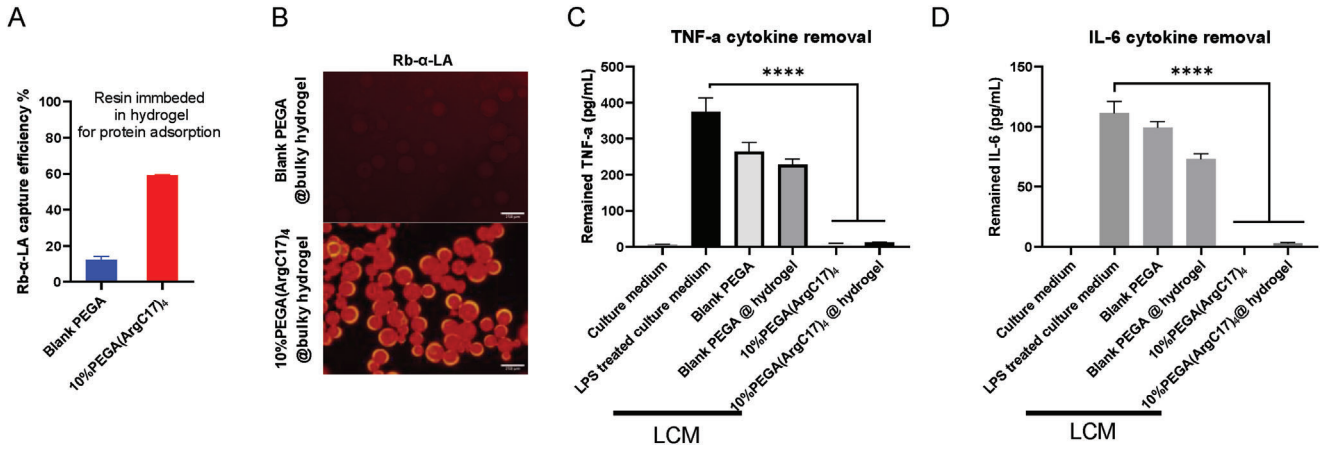

Figure 5. Bulky hydrogel with engineered PEGA-NT enriches its topical applications. Protein capture property of 10% PEGA(ArgC17)$_4$ immobilized in PEG hydrogel at 20% weight ratio was characterized using Rb-α-LA. A) Protein capture efficiency and B) microscopic fluorescent images of blank PEGA and 10% PEGA(ArgC17)$_4$ resins embedded in bulky hydrogel for Rb-α-LA adsorption after 8 h incubation. Scale bar : 250 µm. C) TNF-α and D) IL-6 cytokine removal efficiency was quantified using ELISA after incubating bulky hydrogel only, PEGA-NT resins only, PEGA-NT@hydrogel with LPS-treated cell culture medium for overnight.

2.5. Bulky Hydrogel Embedding PEGA-NT Resin for Topical Application

The PEGA hydrogel resins can be readily functionalized via typical peptide chemistry, however, PEGA-NT resins need to be further formulated in ointment, lotion, or hydrogel for topical application. We chose biocompatible PEG hydrogel as a blank carrier for PEGA-NT resins. PEGA-NT resins can be immobilized in bulky PEG-diacrylate (PEGDA, MW: 6 kDa, 10% aqueous solution) hydrogel before photo-initiated gelation. The bulky hydrogel has pore sizes for biological molecules to diffuse and captured by PEGA-NT resins. Fluorescently labeled Rb-α-LA was used to evaluate the efficiency of resin-in-gel system for protein capture in solution. 10% PEGA(ArgC17)$_4$ resins were immersed in PEGDA hydrogel at 20% weight ratio for protein adsorption and blank PEGA resin was applied as control. The cured bulky hydrogel was fully swollen prior to incubation with the protein to avoid passive solute adsorption during hydrogel swelling. 10% PEGA(ArgC17)$_4$@hydrogel captured 60 µg of protein per 20 mg of resin, while blank PEGA@hydrogel and blank hydrogel controls captured minimal amounts of protein (10 µg) via passive diffusion. Fluorescence microscopy (**Figure 5**B) demonstrated that the engineered 10% PEGA(ArgC17)$_4$ embedded in the hydrogel effectively adsorbed proteins in bulky hydrogel. In contrast, low fluorescence was observed in blank PEGA embedded bulky hydrogel. These data suggest that the bulky hydrogel does not impact the protein capture capacity of TD NT resins.

Using an LPS challenged RAW 264.7 cell culture medium (LCM), we tested the ability of PEGA-NT@hydrogel to capture cytokines. As demonstrated in Figure 5C,D, both 10% PEGA(ArgC17)$_4$@hydrogel and 10% PEGA(ArgC17)$_4$ resin alone efficiently removed proinflammatory cytokines TNF-α and IL-6 from the cell culture medium almost quantitatively. It suggests that the bulky hydrogel scaffold does not restrict the PEGA-NT resins for scavenging cytokines. Control groups, including blank PEGA resin and blank PEGA@hydrogel, showed limited cytokine removal by passive diffusion. This data suggests the feasibility of resin incorporation into other carriers, such as cream, lotion, or ointment for topical therapeutics delivery/scavenging without compromising the efficiency.

2.6. Biocompatibility of Engineered PEGA-NT Resin for Bio-Scavenging

There is a general concern whether broad-spectrum scavenging may deplete essential nutrient/signaling molecules that potentially hinder the cell viability and may result in undesirable side effects. To address this concern, cell culture medium was pre-incubated with PEGA-NT resin of 50 and 100 mg mL^{-1} overnight before adding it to normal cell culture. Then, cell viability assay was conducted after 72 h cell culture as depicted in **Figure 6**A. Mouse immune cell line RAW 264.7 cells and human fibroblast cell line HFF-1 were applied as model cells. Serum-reduced medium (2% FBS) and serum free medium (0% FBS) were applied as positive controls in cell culture, which demonstrated a significant reduction in cell viability to ≈50% due to the reduced nutrient and growth factors. Regardless of the type and concentration of the PEGA-NT resins applied to prime the medium, no significant difference in RAW 264.7 cell and HFF-1 cell viability was observed (Figure 6B,C). This data suggests that the engineered PEGA-NT resins do not adsorb essential and abundant protein from serum, and there is minimum impact on normal cell nutrients and signaling.

2.7. Inflammation Control Effect of Engineered PEGA-NT Resin In Vivo

A preliminary study was performed to assess the immune regulatory capabilities of PEGA-NT resins in an LPS-induced local inflammation mouse model. In this model, LPS solution and PEGA-NT resins were subcutaneously injected into the dorsum of wild type C57BL/6 mice, blank resin co-injected with LPS were

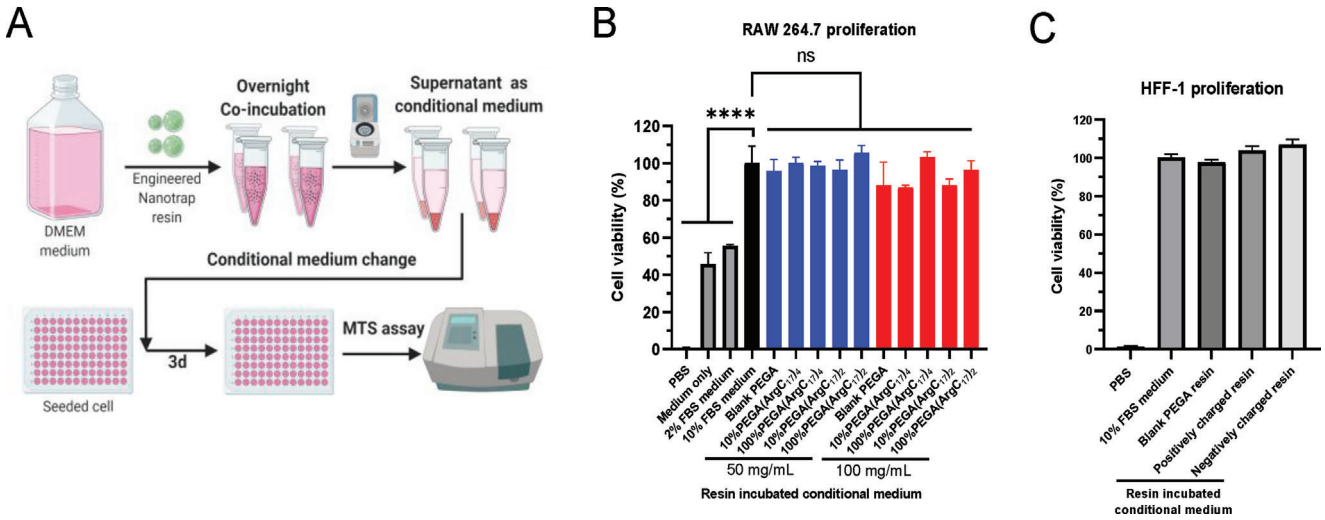

Figure 6. Safety profile of engineered PEGA-NT resin. A) Experimental protocol for the conditional medium incubation cell viability assay. The conditional medium was obtained by incubating TD NT resin with complete DMEM medium (10% FBS and 1% penicillin-streptomycin) overnight, followed by supernatant collection. Cells were then incubated with the conditional medium in a 96-well plate for three days, after which cell viability was determined using an MTS assay. Cell viability of B) RAW 264.7 and C) HFF-1 was normalized to that of complete DMEM medium.

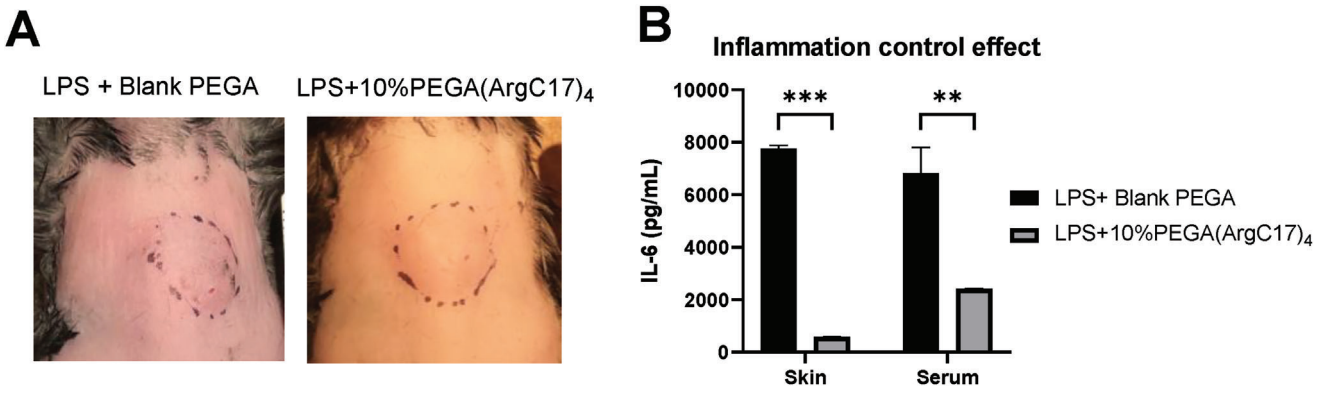

Figure 7. Local deposition of PEGA-NT resins inhibits LPS-induced skin tissue inflammation and prevents systematic hyperinflammation. A) Photo after co-deposition of LPS solution and resin formulations through the same injection sites. Each wild type C57BL/6 mouse was given by two injections at two separate spots. B) Inflammation control effect of engineered PEGA-NT resin was evaluated by IL-6 level in skin tissue homogenate and serum 4 h after injection.

included as control, as shown in **Figure 7**A. After 4 h, we sacrificed the mice and collected serum and injection-site skin tissue for cytokine analysis. Figure 7B showed the significantly attenuated IL-6 in both skin homogenate and serum by the treatment with 10% PEGA(ArgC17)$_4$ resin. This could be attributed to the locally resided PEGA-NT resins scavenge LPS, restricting its diffusion into the bloodstream, and acting as cytokine scavengers that capture locally secreted cytokines.

3. Conclusion

In this study, we optimized the TD NT hydrogel resin by engineering the valency and density of TD in the resin for adsorption of small–medium sized cytokines for topical immune modulation. The reduced TD density in resin results in superior swelling property, better protein capture capacity, and proinflammatory cytokine scavenging effect. The introduction of negatively charged moieties in the TD enables the TD resin to target anti-inflammatory cytokines. Further, the incorporation of functional resins with biocompatible hydrogel as a scaffold enables the application for topical wound dressing, thereby expanding its potential applications. The local deposition of engineered TD NT hydrogel resin shows effective in vivo inflammation control effect. In this context, the results indicated the TD NT hydrogel resins as a promising therapeutic approach in immune modulation for topical chronic wound treatment.

4. Experimental Section

Materials: All chemicals were used as received unless otherwise specified. Amino PEGA resin (Novabiochem, Darmstadt, Germany) was obtained from EMD Millipore (Billerica, MA). (Fmoc)-Lys(Boc)-OH, (Fmoc)-Lys-(Fmoc)-OH, and trifluoroacetic acid (TFA) were obtained from ChemImpex International, Inc. (Wood Dale, IL).

(Fmoc)-Arg(Pbf)-OH was purchased from AnaSpec Inc. (San Jose, CA). Heptadecanoic acid (C17, +98%) was purchased from TCI. *N, N′*diisopropylcarbodiimide (DIC), *N*-hydroxybenzotriazole (HOBt), succinic anhydride, *N, N*-dimethylformamide, anhydrous (DMF, 99.8%), methylene chloride (DCM), methanol (MeOH), and dimethyl sulfoxide (DMSO) were received from Acros Organics (Belglum, NJ). Triethylamine (TEA), α-lactalbumin (α-LA from bovine milk), LPS from *Escherichia coli* (L4130), and *Pseudomonas aeruginosa* (L9143) were purchased from Sigma–Aldrich (St. Louis, MO). Sodium dodecyl sulfate (SDS, +98%) was obtained from Alfa Aesar. ELISA kits were purchased from companies for direct use (interleukin-6, Cat. #: BMS603-2 from Invitrogen, and tumor necrosis factor-α (TNF-α): Cat. #: BMS607HS from Invitrogen). Tetrazolium compound [3-(4,5-dimethylthiazol-2-yl)-5-(3carboxymethoxyphenyl)-2-(4-sulfophenyl)-2H-tetrazolium, MTS] and phenazine methosulfate (PMS) were purchased from Promega (Madison, Wisconsin). Lithium phenyl-2,4,6-trimethylbenzoylphosphinate was purchased from TCI chemicals.

Synthesis of Telodendrimer Nanotrap Resin: The synthesis of NT resin followed a published procedure.[24] As shown in Scheme S1 (Supporting Information), commercial PEGA resin was used as the starting material for NT synthesis, DIC and HOBt were used as catalytic coupling reagents. All reagents were in three-fold excess to the amine functional group on resin. The branched oligolysine scaffold was synthesized by sequential conjugation of (Fmoc)-Lys(Fmoc)-OH. Introduction of guanidine group to the periphery of NT by (Fmoc)-Arg(Pbf)-OH conjugation leads to the production of positively charged resin; introduction of carboxy acid group to the periphery of NT by succinic anhydride generates the negatively charged resin. De-Fmoc was carried out in 20% 4-methylpiperidine DMF solution for 30 min. Pbf- protecting group was removed in the presence of TFA/DCM (50/50, v/v) for 30 min. After reaction completion, residual reactants were removed under vacuum and washed with DMF, DCM, and MeOH for three times each. The heptadecanoic acid was conjugated to the primary amine on the periphery of NT dendron, serving as the hydrophobic moieties. Kaiser test was used to confirm the completion of amid coupling reactions: dark blue indicates the presence of primary amine; yellow color indicates the completion of amine coupling.

Engineering of Telodendrimer Nanotrap Resin: As shown in the inlet table in Scheme S1 (Supporting Information). PEGA resin was engineered before the NT synthesis. The resin was engineered from density and valency. For terminology, the engineered NT resin was named in the format of (density) PEGA$(ArgC_{17})_{\#valency}$, i.e., 10% PEGA$(ArgC_{17})_2$ indicates 10% of free amino groups on the commercial PEGA resin ($\approx$0.33 mmol g^{-1}) was conjugated by bi-valent TD NT. To modify the density (amino loading capacity) to 1%, 5%, 10%, 25%, 50%, and 100%, PEGA resin was reacted with a mixture of Fmoc-Glycine-OH and Boc-Glycine-OH at the predetermined ratios, i.e., 99:1, 95:5, 90:10, 75:25, 50:50, and 0:100, respectively. After conjugation, Fmoc protection groups were removed by the treatment with 20% 4-methylpiperidine DMF solution for 30 min, then free deprotected amine groups were permanently blocked by acetic anhydride. Then Boc-deprotection was conducted via TFA/DCM (50/50, v/v) treatment for 30 min. PEGA resins with reduced amino density were obtained for further TD conjugation. To modify the TD valency, bivalent NT resin was synthesized by single lysine branching conjugation, resulting in one branched NT scaffold. Tetravalent NT resin was synthesized by two consequent conjugations of oligolysine branching, resulting in two layers of branched NT structure.

Quantification of Amine Group Downscaling in PEGA Resin: The downscaling of density of amine groups in PEGA resin could be quantified by UV–vis spectroscopy using the characteristic wavelength of the Fmoc group at 301 nm. Preparation of the PEGA resin sample: a small amount of PEGA resin was taken and washed with solvents, including DMF, DCM, and MeOH to remove any impurities or residual solvents. The resin was then reacted with a mixture of Fmoc-Glycine-OH and Boc-Glycine-OH at the predetermined ratios for overnight, followed by thorough washing procedure with DMF, DCM, and MeOH. The same volume of DeFmoc solution was reacted with resins for at least 30 min. Then the absorbance of the supernatant was measured at 301 nm using a UV–vis spectrophotometer. The absorbance at this wavelength was proportional to the density of the Fmoc group on the resin, which in turn was proportional to the density of the amine groups on the resin. By using this method, the density of amine groups on PEGA resin could be accurately quantified and downscaled as per the requirement. To acquire a standard curve of Fmoc, a known amount of Fmoc-OSu was reacted with DeFmoc solution and quantified by UV–vis spectroscopy.

Evaluation of the Swelling Property of Engineered PEGA-NT Resin: After being synthesized, the resins underwent a rigorous cleaning process, followed by lyophilization and weighing in a dry state (W_{dry}). The dry resins were then soaked in a phosphate-buffered saline (PBS) solution overnight to ensure complete swelling, after which the liquid portion was drained using a vacuum. To ensure thorough liquid removal, the swollen resin was then centrifuged in a filtered column. The swollen resins were weighed in a wet state (W_{wet}), and the soaking-draining-centrifuging process was repeated three times for accuracy. The swelling ratio was calculated as W_{wet}/W_{dry}.

The PEGA resin samples with different densities of TD were soaked in two different solvents, DMSO (dimethyl sulfoxide) and water, to study their swelling behavior. After thorough soaking, the swollen PEGA resin samples were placed on a microscope slide for imaging. Using a microscope equipped with a camera, at least three different fields of view were randomly chosen for each swollen PEGA resin sample in each solvent. The microscope images were then analyzed using image analysis software to manually label the periphery of each resin particle in the image. The diameter of each resin particle was calculated based on its perimeter, and its volume was calculated based on the assumption of a spherical shape. For each solvent and PEGA resin sample, the diameter and volume of at least 150–300 resin particles were measured to obtain a statistically significant sample size. The volume-based average diameter was then calculated by averaging the diameters of all the resin particles in the sample and taking the cube root of the result.

Protein Capture Studies: A-lactalbumin (α-LA) and lysozyme were conjugated with fluorescence for detection purpose. The engineered NT resins were weighted in the Eppendorf tubes. For the capture kinetics experiment, 300 µL of protein solution (1 mg mL^{-1}) was added into each pre-weighted resin-containing tubes (30 mg wet resin), which were then placed on a rotator (set at 10 rpm) under light-protecting aluminum foil cover at room temperature. At each of the pre-determined timepoints, the tubes were spined and the fluorescence of the unabsorbed amount of protein in the supernatant was measured with fluorescence spectrometry in a plate-reader (synergy H1). The fluorescence of the original protein solution served as the starting point. Rb-labeled protein was measured at excitation/emission wavelength of 525/586 nm. Cy3 labeled protein solution was measured at excitation/emission wavelength of 480/570 nm.

The remained protein percent (%) and capture capacity (µg/mg) was calculated by the following formula:

$$\text{Remained protein percent } (\%) = \text{RFU}_{\text{remained}}/\text{RFU}_{\text{original}} * 100 \quad (1)$$

$$\text{Capture capacity } (\mu g/\text{mg}) = \left(\text{RFU}_{\text{original}} - \text{RFU}_{\text{remained}}\right)/\text{RFU}_{\text{original}} * \text{CV/m} \quad (2)$$

where $\text{RFU}_{\text{original}}$ and $\text{RFU}_{\text{remained}}$ are the fluorescence measurement value before and after protein incubation; *C* and *V* are the concentration (µg/mL) and volume (mL) of protein solution, *m* is the wet weight (mg) of the resin.

Protein capture study using PEGA-NT resin embedding in PEG-diacrylate (PEGDA) hydrogel: various weights of 10% PEG$(ArgC17)_4$ wet resin was mixed with PEGDA (10 wt.%) with photoinitiator lithium phenyl-2,4,6-trimethylbenzoylphosphinate (0.1 wt.%) solution. In 48-well plate, 100 µl of such solution was added into wells and irradiated by 405 nm to form PEG bulky hydrogel. The circular resin-embedded PEG hydrogel was taken out to immerse into 200 µL sterile PBS for overnight to achieve totally swollen status. After swelling, the hydrogel was washed with 500 µL PBS, adsorbed to remove excessive liquid, and incubated with Rb-α LA protein solution. The fluorescence intensity of protein solution before, during and

after incubation was measured to quantify the protein capture property. Blank PEG hydrogel and blank PEGA@PEG hydrogel served as controls.

Confocal Microscopy of Engineered PEGA-NT Resin: Fluorescein isothiocyanate (FITC) labeled PEGA resin (PEGA-FITC) was prepared at a swollen status at microscopy slides. Confocal images were acquired with Nikon confocal microscope, FITC laser was used to scan the engineered PEGA-FITC resin. *Z* stack serial images were obtained by layer-by-layer scanning with a setup of 200 µm range and 5 µm interval. *Z* stack movie was automatically generated by Nikon confocal software. Among series of *z* stack serial images, the *xy* plane with an optimal focus was chosen for figure presentation, representative *xz*, and *yz* planes were chosen to demonstrate the homogeneous conjugation of FITC molecules in resin hydrogel network.

Agarose Gel Electrophoresis: Modified from the published assay,[24] the Cy3-α LA loaded NT resins were rinsed once with flash PBS wash to remove un-adsorbed protein solution. Cy3-α LA@NT PEGA resin (2 mg) were loaded into the wells of agarose gel for electrophoresis analysis. Free Cy3-αLA (10 µg) served as a positive control. The electrophoresis was carried out in 1.5% agarose gel at a constant current of 45 mA for 30 min. The gel was imaged by a Bio-Rad ChemiDoc MP imaging system under Cy3 application mode.

Cytokine Removal Study from Culture Medium: *DAMP Generation*: Pancreatic tumor cells Panc-02 were sonicated by primer sonicator, the sonicated cell suspension was centrifuged to harvest the supernatant, serving as the DAMPs- resource.

DAMP/LPS Stimulated Cell Culture Medium: RAW 264.7 cells were seeded in complete Dulbecco's modified Eagle's medium (DMEM) (10% fetal bovine serum (FBS) and 1% penicillin-streptomycin) in a 100 mm culture Petri dish at a 90% confluency. After overnight incubation for cell settling, Panc-02 source DAMP (100 µg mL^{-1}), or endotoxin lipopolysaccharide from *E. Coli* (50 ng mL^{-1}) was added to stimulate macrophage cells in culture for 24 h. Culture medium without DAMP or LPS stimulation were collected as controls. The cell culture medium was centrifuged to remove cell debris and stored at −80 °C freezer for further use.

Cytokine Removal: The proinflammatory cytokine (500 µL) enriched culture supernatant was aliquoted into Eppendorf tubes containing 50 mg of pre-weighted wet NT resins and vortexed to ensure sufficient resin-solution contact. The Eppendorf tubes were rotated at 10 rpm for overnight at 4 °C cold room. The supernatant was collected after centrifugation for ELISA and SDS-PAGE analysis.

Enzyme-Linked Immunosorbent Assay (ELISA): The levels of proinflammatory cytokines tumor necrosis factor-α (TNF-α) and interleukin-6 (IL-6) were measured by ELISA according to manufacturer's instruction. All the cell culture medium samples treated by different NT resins were five times diluted. LPS stimulated cell culture medium without resin incubation served as the positive control, and cell culture medium without LPS stimulation was used as the negative control. Three replicates were included for each sample. Two independent experiments were conducted with consistent results.

Silver Stained SDS-PAGE: Polyacrylamide gel was made with 10-well comb and 1 mm spacer. The wells were loaded with the culture supernatant obtained by incubating engineered NT resins with proinflammatory cytokine enriched cell culture medium. Original culture medium without resin incubation served as the positive control. Electrophoresis was carried out at 80 V for 25 min, followed by 120 V for 70 min. Silver staining was performed following a standard protocol.[34] The gel was imaged by a Bio-Rad ChemiDoc MP imaging system under silver stain mode. Two independent experiments were conducted with consistent results.

Cell Culture and Cell Viability Study: Mouse macrophage RAW 264.7 cells and mouse pancreatic cancer cells Panc-02 (ATCC) were cultured in complete DMEM medium (10% FBS, 1% penicillin-streptomycin, and p/s) at 37 °C in a humidified 5% CO_2 incubator. In 96-well plate, 6×10^3 RAW 264.7 cells per well were seeded and cultured overnight to allow attachment. Meanwhile, 25 or 50 mg of sterilized wet NT resins were incubated with 0.5 mL of complete DMEM medium in Eppendorf tubes for overnight at 4 °C. The conditional medium (without resin) was used to culture the attached cells. Complete DMEM medium (10% FBS and 1% penicillin-streptomycin), serum-reduced DMEM medium (2% FBS and 1% penicillin-streptomycin), DMEM medium only, and PBS were used as control groups. After 72 h, MTS reagents were added to each well according to manufacturer's instructions and the published assay.[24] The absorbance at 490 nm of each well was measured immediately after MTS reagents were added (T_0) and 2 h later (T_2) with a microplate reader (BioTek Synergy 2). The difference in OD490 between T_2 and T_0 was calculated and used to determine the cell viability. The viability was normalized to that of positive control (complete DMEM medium), and was shown as the average cell viability of triplicate wells via a formula of $[(OD - OD_{negative})/(OD_{positive} - OD_{negative}) \times 100\%]$.

Anti-Inflammation Effect of Engineered PEGA-NT Resin In Vivo: C57BL/6J mice (Jackson lab) were maintained under pathogen-free conditions (22 ± 2 °C and 60% air humidity,12 h light/dark cycle) according to the AAALAC (Association for Assessment and Accreditation of Laboratory Animal Care) guidelines and were allowed to acclimatize for at least 4 days before any experiments. All animal experiments were performed in compliance with the institutional guidelines and according to the protocol approved by the Committee for the Humane Use of Animals of State University of New York Upstate Medical University (IACUC # 490). Female C57BL/6J mice were used to study the anti-inflammatory effect of engineered PEGA-NT resin after co-treatment with LPS (*E. Coli*, 5 µg per injection site for mice with 20 g body weight). Blank PEGA resin treatment served as a control group. Each mouse received two injections which were located separately by 2 cm. The dorsum of the mouse was shaved carefully and depilated with hair-removal lotion. LPS solution (50 µL) was mixed with 20 mg of sterilized wet resin and immediately injected subcutaneously using an 18 gauge needle in mice anesthetized with isoflurane. Mice were immediately transferred to individually ventilated cages. Four hours after injection, the mice were sacrificed. The skin tissue near the injection site (pre-labeled), and serum were harvested for cytokine analysis.

Statistical Analysis: For the protein diffusion kinetics study, the data were plotted by GraphPad Prism with an appearance of "Mean and Error" and SD of each replicate measurement was also plotted. Data were presented as means ± SDs in bar graphs, including cytokine removal studies, and cell viability studies. Four parameters logistic (4PL) curve was used to fit and analyze the data obtained from TNF-α and IL-6 ELISA bioassays. The level of significance in all statistical analyses was set at a probability of $P<0.05$. Statistical analysis was performed by two-way analysis of variance (ANOVA) for multiple groups, followed by Šídák's multiple comparisons test.

Supporting Information

Supporting Information is available from the Wiley Online Library or from the author.

Acknowledgements

The authors thank Dr. Samuel Herberg and Dr. Norifumi Urao for their helpful suggestions in the experimental design. The authors acknowledge the financial support from the NIH/NIGMS 1R01GM130941-01, DoD PRMRP/TTD award PR221368, NIH/NHLBI 1 R42 HL166050-01A1, New York Fund for Innovation in Research and Scientific Talent (FIRST), and Maureen T. O'Hara TEAL THERE's A CURE and Christine Schoeck Blakely Ovarian Cancer Research Foundation.

Conflict of Interest

The authors declare no conflict of interest.

Author Contributions

X.Y. conducted the experiments, analyzed the data, and wrote the manuscript. D.G. and X.J. contributed to hydrogel resin synthesis and engineering. C.S. contributed to in vitro and in vivo bioassays. J.L. designed

and supervised the project and revised and finalized the manuscript for publication.

Data Availability Statement

The data that support the findings of this study are available in the supplementary material of this article.

Keywords

bio-scavenging, immune modulation, size exclusive hydrogels, telodendrimer nanotraps, wound healing

Received: June 2, 2023
Revised: July 25, 2023
Published online:

[1] S. A. Eming, P. Martin, M. Tomic-Canic, *Sci. Transl. Med.* **2014**, *6*, 265sr6.
[2] S. Guo, L. A. Dipietro, *J. Dent. Res.* **2010**, *89*, 219.
[3] A. M. Szpaderska, L. A. Dipietro, *Surgery* **2005**, *137*, 571.
[4] S. A. Eming, T. Krieg, J. M. Davidson, *J. Invest. Dermatol. Symp. Proc.* **2007**, *127*, 514.
[5] A. Sindrilaru, T. Peters, S. Wieschalka, C. Baican, A. Baican, H. Peter, A. Hainzl, S. Schatz, Y. Qi, A. Schlecht, J. M. Weiss, M. Wlaschek, C. Sunderkötter, K. Scharffetter-Kochanek, *J. Clin. Invest.* **2011**, *121*, 985.
[6] N. Lohmann, L. Schirmer, P. Atallah, E. Wandel, R. A. Ferrer, C. Werner, J. C. Simon, S. Franz, U. Freudenberg, *Sci. Transl. Med.* **2017**, *9*, aai9044.
[7] M. Kandhwal, T. Behl, S. Singh, N. Sharma, S. Arora, S. Bhatia, A. Al-Harrasi, M. Sachdeva, S. Bungau, *Am. J. Transl. Res.* **2022**, *14*, 4391.
[8] P. P. G. Mulder, M. Vlig, B. K. H. L. Boekema, M. M. Stoop, A. Pijpe, P. P. M. Van Zuijlen, E. De Jong, B. Van Cranenbroek, I. Joosten, H. J. P. M. Koenen, M. M. W. Ulrich, *Front. Immunol.* **2020**, *11*, 621222.
[9] J. W. Penn, A. O. Grobbelaar, K. J. Rolfe, *Int. J. Burns Trauma* **2012**, *2*, 18.
[10] S. Liarte, Á. Bernabé-García, F. J. Nicolás, *Cells* **2020**, *9*, 306.
[11] N. Lian, T. Li, *Biomed. Pharmacother.* **2016**, *84*, 42.
[12] J. P. Andrews, J. Marttala, E. Macarak, J. Rosenbloom, J. Uitto, *Matrix Biol.* **2016**, *51*, 37.
[13] B. Berman, A. Maderal, B. Raphael, *Dermatol. Surg.* **2017**, *43*, S3.
[14] M. K. Lichtman, M. Otero-Vinas, V. Falanga, *Wound Repair Regen.* **2016**, *24*, 215.
[15] J. D. Ference, A. R. Last, *Am. Fam. Physician* **2009**, *79*, 135.
[16] C. T. Turner, S. J. P. McInnes, A. J. Cowin, *Wound Practice & Research: Journal of the Australian Wound Management Association* **2015**, *23*, 16.
[17] K. Zhang, C. Yang, C. Cheng, C. Shi, M. Sun, H. Hu, T. Shi, X. Chen, X. He, X. Zheng, M. Li, D. Shao, *ACS Appl. Mater. Interfaces* **2022**, *14*, 26404.
[18] Y. E. Kim, J. Kim, *ACS Appl. Mater. Interfaces* **2021**, *14*, 23002.
[19] X. Huang, D. He, Z. Pan, G. Luo, J. Deng, *Mater. Today Bio* **2021**, *11*, 100124.
[20] T. Liu, G. Liu, J. Zhang, Z. Ding, Y. Li, K. Sigdel, X. Wang, H. Xie, *Chin. Chem. Lett.* **2022**, *33*, 1880.
[21] C. Shi, D. Guo, K. Xiao, X. Wang, L. Wang, J. Luo, *Nat. Commun.* **2015**, *6*, 7449.
[22] X. Wang, C. Shi, L. Zhang, A. Bodman, D. Guo, L. Wang, W. A. Hall, S. Wilkens, J. Luo, *Biomaterials* **2016**, *101*, 258.
[23] L. Wang, C. Shi, X. Wang, D. Guo, T. M. Duncan, J. Luo, *Biomaterials* **2019**, *215*, 119233.
[24] C. Shi, X. Wang, L. Wang, Q. Meng, D. Guo, L. Chen, M. Dai, G. Wang, R. Cooney, J. Luo, *Nat. Commun.* **2020**, *11*, 3384.
[25] X. Ji, X. Yang, C. Shi, D. Guo, X. Wang, J. M. Messina, Q. Meng, N. Urao, R. N. Cooney, J. Luo, *Adv. Ther.* **2022**, *5*, 2200127.
[26] M. Meldal, F.-I. Auzanneau, O. Hindsgaul, M. M. Palcic, *J. Chem. Soc., Chem. Commun.* **1994**, 1849.
[27] J. H. Petropoulos, A. I. Liapis, N. P. Kolliopoulos, J. K. Petrou, N. K. Kanellopoulos, *Bioseparation* **1990**, *1*, 69.
[28] E. Riccardi, J.-C. Wang, A. I. Liapis, *J. Chem. Phys.* **2010**, *133*, 084904.
[29] K. T. Xenaki, S. Oliveira, P. M. P. Van Bergen En Henegouwen, *Front. Immunol.* **2017**, *8*, 1287.
[30] S. Ellis, E. J. Lin, D. Tartar, *Curr. Dermatol. Rep.* **2018**, *7*, 350.
[31] R. C. Switzer, C. R. Merril, S. Shifrin, *Anal. Biochem.* **1979**, *98*, 231.
[32] A. Yoshimura, Y. Wakabayashi, T. Mori, *J. Biochem.* **2010**, *147*, 781.
[33] M. R. Bootcov, A. R. Bauskin, S. M. Valenzuela, A. G. Moore, M. Bansal, X. Y. He, H. P. Zhang, M. Donnellan, S. Mahler, K. Pryor, B. J. Walsh, R. C. Nicholson, W. D. Fairlie, S. B. Por, J. M. Robbins, S. N. Breit, *Proc. Natl. Acad. Sci. U. S. A.* **1997**, *94*, 11514.
[34] J. M. Kavran, D. J. Leahy, *Methods Enzymol.* **2014**, *541*, 169.